Pyrometallurgical copper smelting scheme of chalcocite: thermodynamic theoretical analysis and experimental verification of direct-to-blister smelting method using chalcocite mixed with pyrite

SONG WANG[1], GUOZHI LV [1,*], TINGAN ZHANG[1]

1.—Key Laboratory of Ecological Metallurgy of Multi-metal Intergrown Ores of Ministry of Education, School of Metallurgy, Northeastern University, Shenyang, China.

*Corresponding e-mail: lvgz@smm.neu.edu.cn

Abstract

Chalcocite ore, which has high silica but low iron contents, is uneconomical to smelt using conventional two stage smelting processes. In this paper, thermodynamic analysis and experimental verification of the direct-to-blister smelting of chalcocite ore were studied. The equilibrium compositions, slag phase diagrams and slag viscosities indicated that the direct-to-blister smelting of chalcocite ore is unreasonable, and the thermodynamic adjustment scheme shows that adding pyrite and calcium oxide to the chalcocite ore can make the slag type reasonable. The feasibility control plan of the slag type was verified by experiments, and the experimental data were analyzed by chemical composition analysis, XRD, EPMA and viscosity measuring apparatus. The experimental results are in good agreement with the theoretical calculations. The copper recovery is between 80% and 91%, while the content of copper in the slag is in the range of 8% to 15%, indicating that direct-to-blister smelting can be realized on a lab scale.

Keywords: Chalcocite, Pyrite, Direct-to-blister smelting, thermodynamic analysis, experimental verification

1. Introduction

The extractive metallurgy of copper can be divided into two group processes, namely, pyro-metallurgy and hydrometallurgy, and the former is dominant. According to recent data, about 10% of copper is produced through continuous converting processes, such as flash converting. The remainder of the pyrometallurgical production comes from both PSCs (primary smelting converters) and other discontinuous converting processes. The first stage of the conventional copper pyro-metallurgy process is to smelt copper concentrate to copper matte composed of FeS and Cu_2S with slagging to remove partial iron [1]. The smelting processes include bath and flash smelting. The second stage of the process is to convert the copper matte to blister copper [2–4]. In most cases, the copper matte is converted in a P-S converter, and it is a batch operation [5–7]. The remaining 20% of primary copper production comes from hydrometallurgical processing of mainly copper oxide and chalcocite ores [8–11].

Chalcocite (Cu_2S) is one of the main minerals of copper in nature and is characterized by high copper content (the mass fraction of copper in the concentrate produced by beneficiation can reach more than 40%), and low sulfur and iron content. Usually, chalcocite ores are processed by hydrometallurgy, and this method mainly recovers copper through leaching, followed by solvent extraction and electrowinning. However, wet copper refining has problems such as high consumption of chemical reagents, wastewater pollution and waste acid treatment, etc. Although bio-bacterial leaching can reduce some of the above problems, it can not solve the low efficiency inherent in wet copper refining, and also bacterial leaching has the problem of complex control of temperature, aeration, microbial community and other parameters, which can not precisely control the heap leaching process for a long period of time [10]. Due to the characteristics of high copper, low iron and high silicon of chalcocite ore, especially the copper grade in it is close to or higher than the copper matte grade produced by ordinary matte smelting, if the traditional matte smelting-copper matte smelting method is used for copper extraction, it is obviously uneconomical. There are two main problems in the smelting method, one is that the sulfur content of the concentrate is low so that it is impossible to achieve self-heating smelting without external heating, and the other is that the slag type is difficult to stably control and cannot reach the copper content level of conventional copper concentrate smelting slag. Therefore, it is necessary to study the direct-to-blister copper smelting process of high-grade chalcocite ore [12–15].

Compared with the conventional two-step smelting -converting process, direct-to-blister copper smelting process has the following advantages: (a) It generates a single, continuous off-gas with high-concentration SO_2, which is easily collected and highly suitable for acid-making operations; (b) It has lower energy consumption; (c) It requires lower capital expenditure (Capex) and operating expenditure (Opex). D. R. Swinbourne believed that any copper concentrate can generate blister copper by direct smelting in the flash furnace [16]; however, given the economic feasibility, the low grade copper concentrate is not suitable. Hao et al. believed that when the ratio of copper to sulfur is lower than 1.7, the direct to blister copper smelting process is not economical[17]. Wang et al. pointed out that the addition of a certain amount of calcium oxide can decrease slag viscosity, and improve copper recovery through experiments [18,19]. At present, there are three copper smelters using the direct blister copper process, i.e. Glowgow Copper Smelter in Poland, Olympic Dam Smelter in Australia and Chingola Smelter in Zambia.

There are few thermodynamic analyses related to the direct-to-blister copper smelting process. In this study, chalcocite ore is used as a raw material, and the Equilib Module, Phase Diagram Module and Viscosity Module in FactSage software are used to analyze the thermodynamic data of direct-to-blister copper smelting process. The optimal slag type feasibility control experimental scheme calculated by FactSage is experimentally verified, and the theoretical point phase composition is verified and corrected by means of chemical composition analysis, XRD, EPMA and other means. At the same time, smelting parameters such as copper direct yield, blister copper grade, blister copper content, and slag copper content were investigated to verify the feasibility of direct-to-blister smelting from chalcocite ore under laboratory conditions.

2. Materials and Method

2.1 Materials

This paper takes chalcocite ore provided by a copper smelter in Fujian as the research object, and its physical appearance is gray-black solid particles. At room temperature, the chemical analysis was carried out after crushing and grinding. The analysis results are shown in Table 1. The copper content in this chalcocite ore is as high as 53.55%, and the iron, sulfur and silica contents are 4.23%, 15.26% and 14.37%, respectively. In addition to containing a small amount of other gangue components, it belongs to the typical low-iron and high-silicon type chalcocite ore.

2.2 Methods

For the thermodynamic analysis, a series of calculations of the equilibrium compositions, slag phase diagram, and slag viscosity of copper smelting were completed in the thermodynamic simulation software FactSage. The database selections in this study are FactPS, FToxid and FTmisc, and the calculation modules used are Equilib Module, Phase Diagram Module and Viscosity Module. The equilibrium calculation results gave the content of each substance in the gas phase, copper liquid phase and slag liquid phase in detail so that the copper smelting parameters can be calculated. Mathematical expressions for the direct yield of copper (η_C), sulfur content in blister copper (η_S) and blister copper grade (Θ) were defined as follows, where M_C and M_R represent the mass of copper in the copper liquid phase and the raw material, respectively; M_S and M_T are mass of sulfur in copper liquid phase and total mass of copper liquid phase, respectively. Enter the content of the main oxides (SiO_2, CaO, Al_2O_3, MgO, Fe_2O_3, and FeO) in the slag liquid phase obtained by the Equilib Module and the specified temperature in the Viscosity Module, and then the corresponding viscosity data can be obtained. The pseudo-ternary system phase diagrams were drawn by fixing the ratio of Al_2O_3, MgO and Fe_2O_3 and using CaO-SiO_2-FeO as the variable to analyze the influence of the change of iron-silicon ratio and CaO on the composition properties of slag, and to carry out reasonable slag type adjustment.

$$\eta_C = \frac{M_C}{M_R} \tag{1}$$

$$\eta_S = \frac{M_S}{M_T} \tag{2}$$

$$\theta = \frac{M_C}{M_T} \tag{3}$$

For the experimental procedure, first, put the empty crucible (m_1) and the oxygen lance into the constant temperature zone of the electric furnace. Raise the temperature to 1300°C at a heating rate of 10°C/min. Once the temperature is stabilized, maintain it for 30 minutes. After this period, use the feeder to introduce 60 g of material into the crucible. After the charge is completely melted, the oxygen lance is inserted into the bottom of the molten material layer, and oxygen-enriched gas is injected. After the injection was completed, the oxygen lance was pulled out, allowed to stand at 1300 °C for a certain period of time, and then cooled to room temperature with the furnace. The crucible containing the material was removed, and the crucible (m_2) was weighed. The crucible was crushed to take material, the blister copper was separated from the slag, the copper content in the slag (α) was detected, the blister copper mass (m_3) was weighed, and the slag phase quality (m_4) and the copper direct yield (η) were calculated. The calculation method is as follows:

$$m_4 = m_2 - m_1 - m_3 \tag{4}$$

$$\eta = m_3 / (m_4 \times \alpha + m_3) \tag{5}$$

3. Results and discussion

3.1 Thermodynamic analysis

3.1.1 Problems existing in the direct-to-blister copper smelting of chalcocite

When the oxygen-enriched concentration of the injected gas is 70%, the phase equilibrium process of the direct-to-blister copper smelting process for chalcocite is shown in Fig. 1. When the temperature is lower than 1150°C, there is less slag-liq and much SiO_2, spinel, cordierite ($Mg_2Al_4Si_5O_{18}$), $CaAl_2Si_2O_8$, and orthopyroxene in the melt. The slag liquid phase increases with the temperature, and SiO_2, spinel, $Mg_2Al_4Si_5O_{18}$, and $CaAl_2Si_2O_8$ are gradually dissolved in the slag liquid phase, which is good for the separation of blister copper and slag. When the temperature reaches to 1300°C, the SiO_2 phase still exists, but the major phase is slag-liquid. Fig. 1 (b) shows the composition in the slag liquid phase. When the temperature rises from 1100°C to 1200°C, the Cu_2O content in the slag liquid phase increases significantly, corresponding to a declining trend of the amount of blister copper in Fig. 1 (a). With a temperature increase lower than 1250°C, more metallic copper is oxidized into the slag liquid phase, and the copper recovery is reduced. As the temperature increases to a high level, the Cu_2O content in the slag liquid phase increases slowly. The viscosity of direct-to-blister copper smelting slag calculated by FactSage for each oxygen concentration is shown in Table S-1. Under various oxygen concentrations, the viscosity of molten slag at 1250°C and 1300°C is greater than 29 Pa·s, indicating that the direct direct-to-blister smelting of chalcocite slag type is unreasonable and that normal smelting cannot be carried out.

Fig. 2 shows the slag phase diagram, which indicates that the SiO_2 phase precipitated from the slag under smelting conditions. This results in higher slag viscosity and poorer fluidity, thus making operation difficult in the direct blister copper smelting process for chalcocite. To ensure the smooth process of direct-to-blister copper smelting, the smelting slag type needs to be adjusted. In addition, when the temperature rises from 1250 °C to 1300 °C, it can be seen from the phase diagram that the liquid phase area of molten slag expands (yellow area in Fig. 2), indicating that it is easier to control molten slag in high-temperature smelting.

3.1.2 Slag type adjustment

Fig. 3 shows the synthetic diagram of the phase diagram of the copper slag series in the direct direct-to-blister copper smelting of chalcocite at 1300°C under various oxygen concentrations. It can be seen that the change in oxygen concentration has little effect on the phase diagram of the slag system. With increasing oxygen concentration, the slag liquid phase area showed a trend of expansion, the spinel-slag liquid zone showed a downward trend, and the area size showed no obvious change. In the direct direct-to-blister copper smelting process of chalcocite at 1300°C, the SiO_2 phase is precipitated from the slag under smelting conditions, resulting in a higher viscosity of slag, which cannot smoothly step smelting.

According to Fig. 3, the following solutions can be obtained: The iron-silicon ratio and CaO content of the slag were adjusted so that the slag composition point was located in the slag liquid phase region (Fig. 3 yellow area), and the adjustment range of the iron-silicon ratio was less than 1.05. The slag composition point is adjusted to the molten slag liquid phase near the middle region, which is convenient for practical operation.

Table 2 shows the effect of CaO addition on smelting parameters, and slag phase diagrams are shown in Fig.4. When the amount of CaO is 1.2%, the composition point of molten slag just enters the liquid phase of slag, and the viscosity of molten slag is 20.62 Pa •s. Continuing to add CaO, the viscosity of the slag decreases. When the CaO addition amount was 5.2%, the composition point of slag was the central position of the slag liquid phase region, which was beneficial to the actual smelting operation, but the slag viscosity value was still high, which was 2.59 Pa •s. When the content of CaO is 11.1%, the slag component point is the slag liquid phase boundary region, there are more spinel regions in the phase diagram, and the viscosity of slag is 0.69 Pa •s. Therefore, it is more difficult for the direct-to-blister copper smelting process for chalcocite. As the amount of CaO is further increased, solid $CaO•SiO_2$ and melilite will precipitate out of the melt.

It can be seen from the adjustment plan parameters in Table 2 that the direct-to-blister copper smelting of chalcocite has the problem of high S content in blister copper. Fig.5 shows the Cu-S binary phase diagram. When the S in the melt at 1300 °C is reduced to less than 1.63%, the melt is transformed from a copper matte-blister copper two-phase to a blister copper phase. Therefore, it is necessary to further control the slag type. The change in S content in blister copper is mainly affected by the oxygen potential/sulfur potential in the furnace. When the oxygen potential decreases, the sulfur potential increases correspondingly, resulting in an increase in the S content in the blister copper; in contrast, the S content in the blister copper decreases. Therefore, on the basis of the existing conclusions, the amount of oxygen was adjusted appropriately to reduce the S content in blister copper to approximately 0.5%, and the optimal slag type feasibility control scheme for direct-to-blister copper smelting of chalcocite was obtained.

3.1.3 The best slag type feasibility control scheme

The optimal thermodynamic control scheme of the method of adjusting the iron-silicon ratio is shown in Table 3 and 4. The specific smelting parameters are as follows: the slag viscosity is 0.49~0.69 Pa s, the blister copper grade is 99.12~99.36%, the copper direct yield is 88.06 %~95.37%, and the S content in blister copper is stable at approximately 0.5%.

3.2 Verification of Experiment

This section mainly carries out the direct-to-blister copper smelting experimental verification of chalcocite. The experimental results may be inaccurate due to the deviation of each step in the experimental process, such as the low oxygen utilization rate, incomplete settlement of blister copper, high viscosity of slag liquid, etc. Therefore, the effects of the gas injection rate, gas injection time, settling time and calcium oxide addition amount on the smelting parameters of direct-to-blister copper smelting were first discussed through experiments, and then the experimental conditions were optimized. At the same time, the similarities and differences between the experimental results and thermodynamic analysis were compared and analyzed, and the feasibility of direct-to-blister copper smelting from chalcocite was analyzed.

3.2.1 Effect of gas injection time

The amount of oxygen has a crucial influence on the direct yield of copper and the copper content of the slag [20]. Increasing the amount of oxygen can reduce or remove the Cu_2S layer in the melt, but too much oxygen will also cause no Cu_2S layer in the melt to reduce Cu_2O, which leads to an increase in the copper content of the slag. The injection time and the injection rate jointly determine the injection oxygen amount. Due to the experimental operation and other reasons, the fixed gas injection rate is 0.4 L/min, so the injection time directly determines the amount of oxygen.

Under the conditions of an experimental temperature of 1300°C, oxygen concentration of 21%, gas injection rate of 0.4 L/min and settling time of 3 h, the influence of injection time on the direct yield of copper was studied. Under this condition, the theoretical injection time is 112 min, and the experimental results are shown in Table 5. With increasing injection time, the direct copper yield showed a trend of increasing first and then decreasing. When the injection time was close to the theoretical injection time, the direct copper yield was greater than 89.2%. When the injection time was 118 min (105.3% of the theoretical injection time), the direct copper yield showed a maximum value of 90.5%. The injection time continued to increase, and the direct yield of copper gradually decreased. When the injection time was 180 min, the blister copper disappeared completely. To prevent the chance of the experiment, another two groups of parallel experiments were performed to ensure rigor, and the experimental results are given in Table S-2 and Table S-3. The experimental results show that when the direct yield of copper reaches the maximum value, the gas injection time is approximately 105% of the theoretical injection time, which is consistent with the conclusion of experiments 1-8.

Taking the slag from Experiments 2, 5 and 6 for XRD analysis, the results are shown in Fig. 6a. When the injection time is 100 min, there are obvious Cu_2S diffraction peaks in the slag XRD pattern, indicating that the reaction is not complete, and there is a Cu_2S layer in the melt, resulting in the direct yield of copper being low. When the injection time was 123 min, Cu_2O diffraction peaks appeared in the XRD pattern of the slag, indicating that the amount of Cu_2O dissolved in the slag increased due to injection overoxidation. When the injection time was 118 min, the copper phase in the XRD pattern of the slag was mainly Cu, and no obvious Cu_2S and Cu_2O diffraction peaks were found, indicating that the reaction was complete and that the amount of injected oxygen was appropriate. Fig. 6b shows the physical map of blister copper in experiment 5. Fig. 6c shows the EPMA surface scan of the slag when the injection time is 118 min. The figure also shows that copper mainly exists in the form of metallic copper in the slag, and the slag type is mainly calcium-silicon slag. Therefore, it is reasonable to think that the injection time should be 105% of the theoretical oxygen injection time.

3.2.2 Effect of sedimentation time

Under the conditions that the experimental temperature is 1300℃, the gas injection rate is 0.4 L/min, and the injection time is 105% of the theoretical injection time, the influence of the copper settling time of adding calcium oxide to chalcocite on the direct yield of copper is studied. Fig. 7 shows the effect of settling time on copper recovery at oxygen concentrations of 21%. It can be seen from the figure that when the sedimentation time was increased from 30 min to 120 min, the copper recovery rate increased significantly, the sedimentation time continued to increase, and the copper recovery rate almost did not increase. Therefore, 120 min is a suitable settling time.

3.2.3 Effect of calcium oxide amounts

Fig. 8a shows the effect of different CaO additions on the direct copper yield, indicating that with the increase in CaO addition, the direct copper yield increases, and as the CaO content increases from 4% to 11.3%, the crude copper yield increases from 65.06% to 90.78%, and the copper content in the slag is reduced from 17.64% to 8.59%. Fig. 6c shows the viscosity curve of the slag with different CaO additions during the direct-to-blister copper smelting experiment of chalcocite. At 1300℃, with the increase in CaO content from 4% to 11.3%, the viscosity value gradually decreased, from 4.006 Pa·s to 1.702 Pa·s, which is consistent with the decreasing trend of the theoretical calculation of adding CaO, but the theoretical calculation of CaO shows that when the content is 11.3%, the viscosity is only 0.70 Pa·s, while the measured value of the viscosity in the actual experiment is 1.702 Pa·s, and the numerical gap is large, which is also the main reason why the actual direct yield of copper is lower than the theoretical direct yield, because copper The loss in the slag is divided into mechanical entrainment and chemical dissolution, but only chemical dissolution is considered in the theoretical calculation [21]. In the experiment, copper inevitably enters the slag phase due to mechanical entrainment, resulting in a decrease in the direct yield.

Fig. 8b shows the XRD patterns of the slag with different CaO additions. When the addition of calcium oxide is 4% and 5%, there is a Cu_2S phase in the slag, and when the addition of calcium oxide exceeds 6%, Cu_2S disappears. This is due to the addition of calcium oxide. Reduce slag viscosity, facilitate melt flow and promote copper formation. Continuing to increase the calcium oxide content, diopside and diopside iron phases are formed in the slag. When the addition amount of calcium oxide is 11.3%, although the amount of slag increases, the dissolved oxygen content in the slag increases, which promotes the oxidation loss of copper, but the viscosity of the system decreases(Fig. 8c), which reduces the loss of copper due to mechanical entrainment. Therefore, considering the factors affecting the direct copper yield, the theoretical calcium oxide addition amount of 11.3% has the best effect.

3.2.4 Verification of Experiment

After the above experimental discussion, the thermodynamic optimal scheme (Table 3) was used for experimental verification. The verification experiment was carried out using 105% of the theoretical oxygen injection time, a 2-hour sedimentation time and the theoretical calcium oxide addition amount. The experimental results and theoretical data are listed in Table 6. The direct yield of copper at each iron-to-silicon ratio is lower than the theoretical value. There are three main reasons. First, in the actual smelting process, some elemental copper will enter the slag phase due to mechanical entrainment, resulting in an increase in the loss of copper in the slag, and this loss quantitative simulation cannot be calculated by thermodynamic theory. Second, the crucible and oxygen lance used in the experiment are made of corundum (Al_2O_3), which will react with copper slag at the experimental temperature (1300°C), resulting in an increase in the Al_2O_3 content in the slag by approximately 120%. The viscosity of the slag increases, and the mechanical loss in the slag further increases.

Technical indicators for direct-to-blister copper smelting by adjusting the iron-silicon ratio of chalcocite mixed pyrite to 0.35, 0.6 and 0.8 are shown in Table 6. In general, in the obtained experimental results, the direct yield of copper is between 80% and 91%, while the content of copper in the slag is in the range of 8% to 15%. The copper grades in the experimentally obtained blister copper are all greater than 98%, which is lower than the theoretically calculated blister copper grade, which is attributed to the theoretical calculation without considering impurity elements (such as arsenic, antimony, bismuth, etc.) in the copper concentrate. The blister copper sulfur content is in good agreement with the theoretical calculated value. The experimental results are in good agreement with the theoretical calculations, indicating that the direct-to-blister copper smelting of chalcocite can be realized under laboratory conditions.

4. Conclusions

In this paper, thermodynamic and experimental studies on the direct-to-blister smelting of chalcocite were conducted. Chalcocite ore has a low iron-silica ratio, and silica would precipitate in the melt at 1300°C. The thermodynamic adjustment scheme shows that adding pyrite and calcium oxide to the chalcocite can make the slag composition point located in the slag liquid phase region. Based on the equilibrium phase composition, slag phase diagram, slag viscosity, and sulfur content in copper, the optimal slag type feasibility control scheme were calculated. The smelting parameters were as follows: the slag viscosity was 0.49~0.69 Pa·s, the blister copper grade was 99.12~99.36%, the copper direct yield was between 88.06%~95.37%, the sulfur content in blister copper was stable at approximately 0.5%.

The verification experiment was carried out using 105% of the theoretical oxygen injection time, a 2-hour sedimentation time and the theoretical calcium oxide addition amount. The results of the verification experiment showed that the copper recovery ranged from 80% to 91%, while the copper content in the slag varied between 8% and 15%. Since the mechanical entrainment loss of copper in the slag could not be calculated theoretically, the experimental copper content in the slag was higher, leading to a lower copper recovery than the theoretical value. The blister copper grade was close to the theoretical value, and the sulfur content in blister copper matched the theoretical value. The experimental results are in good agreement with the theoretical calculations, indicating that direct-to-blister smelting can be realized on a lab scale.

CONFLICT OF INTEREST

The authors declare that they have no conflict of interest.

Acknowledgments

The authors gratefully acknowledge the financial support of this work by the National Natural Science Foundation of China (No. ZX20230386), 2023 Special Project for Industrial Base Reconstruction and High-Quality Development of Manufacturing Industry (No. 2023ZY01019 – 11), Jiangxi Province “Double Thousand Plan” Project (No. S2021DQKJ2198), and The sixth batch of top talent support funds (No. QNBJ-2022-04).

REFERENCES

1. Traulsen, H. R., Taylor, J. C., and George, D. B., “Copper smelting — an overview”, *JOM*, **34**(8), pp. 35–40 (1982). https://doi.org/10.1007/BF03338071
2. Kojo, I. V., Jokilaakso, A., and Hanniala, P., “Flash smelting and converting furnaces: a 50 year retrospect”, *JOM*, **52**(2), pp. 57–61 (2000). https://doi.org/10.1007/s11837-000-0049-5
3. Devia, M., Parra, R., Queirolo, C., et al. “Copper smelting and converting: past and present chilean developments”, *Mineral Processing and Extractive Metallurgy*, **128**(1–2), pp. 108–116 (2019). https://doi.org/10.1080/25726641.2018.1542050
4. Wang, S., Wang, Q., Guo, X., et al. “Operation and fundamentals of direct anode copper production from matte”, *Metall Mater Trans B* (2023). https://doi.org/10.1007/s11663-023-02721-8
5. Matousek, J. W., “The oxidation mechanism in copper smelting and converting”, *JOM*, **50**(4), pp. 64–65 (1998). https://doi.org/10.1007/s11837-998-0272-z
6. Zhao, B. and Liao, J., “Development of bottom-blowing copper smelting technology: a review”, *Metals*, **12**(2), p. 190 (2022). https://doi.org/10.3390/met12020190
7. Zhao, H., Wang, J., Liu, F., et al. “Flow zone distribution and mixing time in a peirce—smith copper converter”, *Int J Miner Metall Mater*, **29**(1), pp. 70–77 (2022). https://doi.org/10.1007/s12613-020-2196-8
8. Feng, Q., Yang, W., Wen, S., et al. “Flotation of copper oxide minerals: a review”, *International Journal of Mining Science and Technology*, **32**(6), pp. 1351–1364 (2022). https://doi.org/10.1016/j.ijmst.2022.09.011
9. Liang, Z., Wang, Q., Tang, L., et al. “Recover of Cu from copper oxide ore using magnetic separation-leaching process and magnetism study of copper-containing minerals”, *Minerals*

Engineering, **218**, p. 109006 (2024). https://doi.org/10.1016/j.mineng.2024.109006

10. Yu, S., Liao, R., Yang, B., et al. “Chalcocite (bio)hydrometallurgy—current state, mechanism, and future directions: a review”, *Chinese Journal of Chemical Engineering*, **41**, pp. 109–120 (2022). https://doi.org/10.1016/j.cjche.2021.12.014
11. Clotilde Apua, M. and Madiba, M. S., “Leaching kinetics and predictive models for elements extraction from copper oxide ore in sulphuric acid”, *Journal of the Taiwan Institute of Chemical Engineers*, **121**, pp. 313–320 (2021). https://doi.org/10.1016/j.jtice.2021.04.005
12. Michal, E. J. and Schuhmann, R., “Thermodynamics of iron-silicate slags: slags saturated with solid silica”, *JOM*, **4**(7), pp. 723–728 (1952). https://doi.org/10.1007/BF03398131
13. Lee, J., Acar, S., Doerr, D. L., et al. “Comparative bioleaching and mineralogy of composited sulfide ores containing enargite, covellite and chalcocite by mesophilic and thermophilic microorganisms”, *Hydrometallurgy*, **105**(3–4), pp. 213–221 (2011). https://doi.org/10.1016/j.hydromet.2010.10.001
14. Fallah-Mehrjardi, A. Hayes, P. C., et al. “The Effect of CaO on gas/slag/matte/tridymite equilibria in fayalite-based copper smelting slags at 1473 K (1200 °C) and P(SO2) = 0.25 atm”, *Metall and Materi Trans B*, **49**(2), pp. 602–609 (2018). https://doi.org/10.1007/s11663-018-1170-6
15. Johansen, E.-B., Rosenqvist, T., and Torgersen, P. T., “On the thermodynamics of continuous copper smelting”, *JOM*, **22**(9), pp. 39–47 (1970). https://doi.org/10.1007/BF03355661
16. Swinbourne, D. R., West, R. C., et al. “Computational thermodynamic modelling of direct to blister copper smelting”, *Mineral Processing and Extractive Metallurgy*, **120**(1), pp. 1–9 (2011). https://doi.org/10.1179/1743285510Y.0000000003
17. Hao, J., Dou, Z., Zhang, T., et al. “Energy conservation and emission reduction through utilization of latent heat of copper slag for iron and copper recovery”, *Journal of Cleaner Production*, **436**, p. 140602 (2024). https://doi.org/10.1016/j.jclepro.2024.140602
18. Madej, P., “Influence of the reduction rate of slag from oxidation process of Cu–Fe–Pb alloy during reduction (de-coppering) on its viscosity”, *Metall Mater Trans B* (2024). https://doi.org/10.1007/s11663-024-03381-y
19. Wang, S., Wang, Q., Guo, X., et al. “Operation and fundamentals of direct anode copper production from matte”, *Metall Mater Trans B* (2023). https://doi.org/10.1007/s11663-023-02721-8
20. Kang, Y., Shin, K.-S., and Morita, K., “Influence of oxygen on Cu distribution behavior between molten Iron and FeS-Based Flux”, *Metall and Materi Trans B*, **49**(3), pp. 944–948 (2018). https://doi.org/10.1007/s11663-018-1225-8
21. Shishin, D., Hidayat, T., Fallah-Mehrjardi, et al. “Integrated experimental and thermodynamic modeling study of the effects of Al2O3, CaO, and MgO on slag–matte equilibria in the Cu-Fe-O-S-Si-(Al, Ca, Mg) system”, *J. Phase Equilib. Diffus.*, **40**(4), pp. 445–461 (2019). https://doi.org/10.1007/s11669-019-00716-0

Figure and table captions

Fig. 1. The effect of temperature on (a) the change in phase composition and (b) the change in phase composition in slag during the direct blister copper smelting process of chalcocite.

Fig. 2. Slag phase diagram at (a) 1250°C and (b) 1300°C.

Fig. 3. Composite phase diagram of the copper slag in the direct-to-blister smelting of chalcocite under various oxygen concentrations at 1300°C.

Fig.4. Slag phase diagram in direct-to-blister copper smelting of chalcocite at 1300 °C with CaO addition of (a) 1.2%, (b) 5.2%, (c) 11.1%.

Fig.5. Phase diagram of Cu-S

Fig. 6. (a) XRD patterns of copper slag obtained in experiments 2, 5, and 6; (b) Physical map of blister copper in experiment 5; (c) EPMA diagram of copper slag in experiment 5.

Fig. 7. Effect of sedimentation time on copper recovery.

Fig.8. (a) The influence of different CaO additions on copper yield; (b) X-ray diffraction pattern of the slags with different CaO additions; (c) Effect of adding different amounts of CaO to chalcocite on the viscosity of molten slag.

Table 1. Chemical composition of chalcocite raw material.

Table 2. The effect of CaO addition on smelting parameters.

Table 3. Chemical composition (%) of the optimal slag type feasibility control scheme.

Table 4. Smelting parameters table of the optimal slag type feasibility control scheme.

Table 5. The effect of gas injection time on copper recovery at a 21% oxygen concentration.

Table 6. Technical indicators for direct-to-blister copper smelting by adjusting the iron-silicon ratio of chalcocite mixed pyrite to 0.35, 0.6 and 0.8.

Figure and table

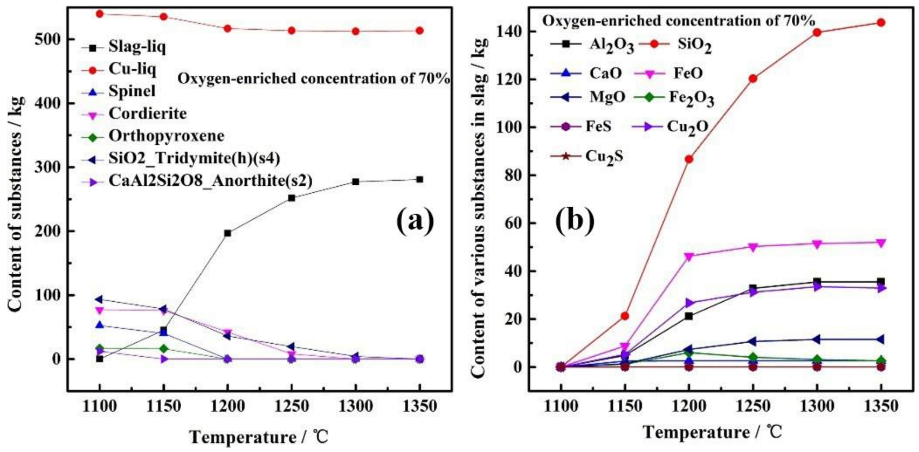

Fig. 1. The effect of temperature on (a) the change in phase composition and (b) the change in phase composition in slag during the direct blister copper smelting process of chalcocite.

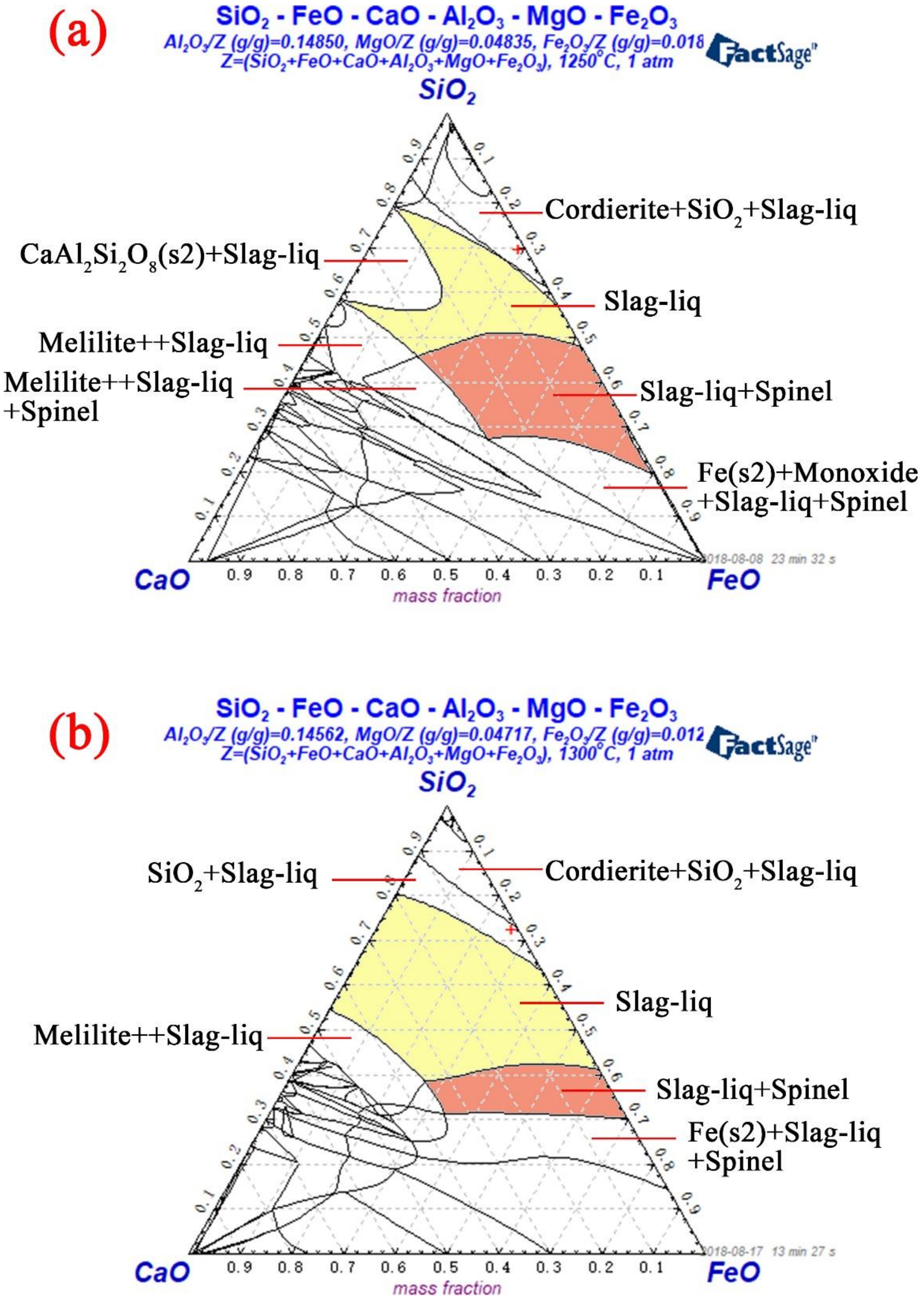

Fig. 2. Slag phase diagram at (a) 1250°C and (b) 1300°C.

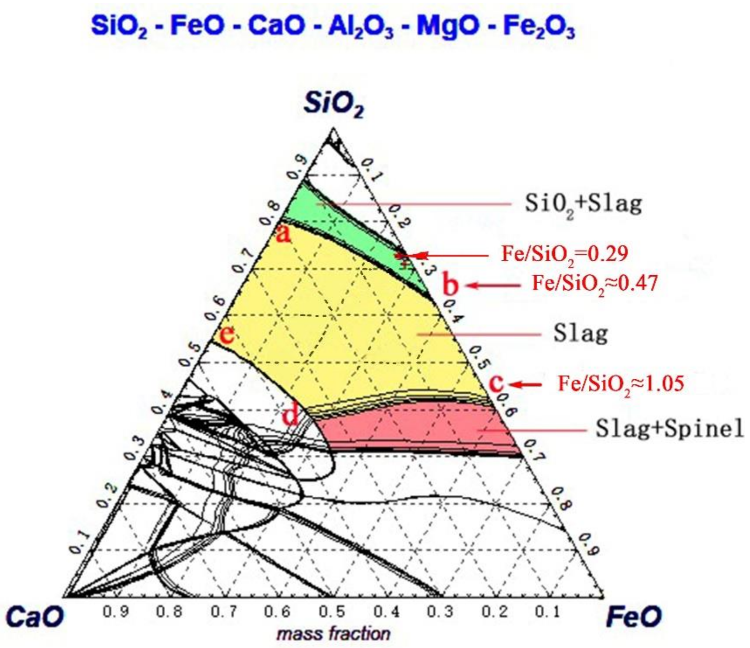

Fig. 3. Composite phase diagram of the copper slag in the direct-to-blister smelting of chalcocite under various oxygen concentrations at 1300°C.

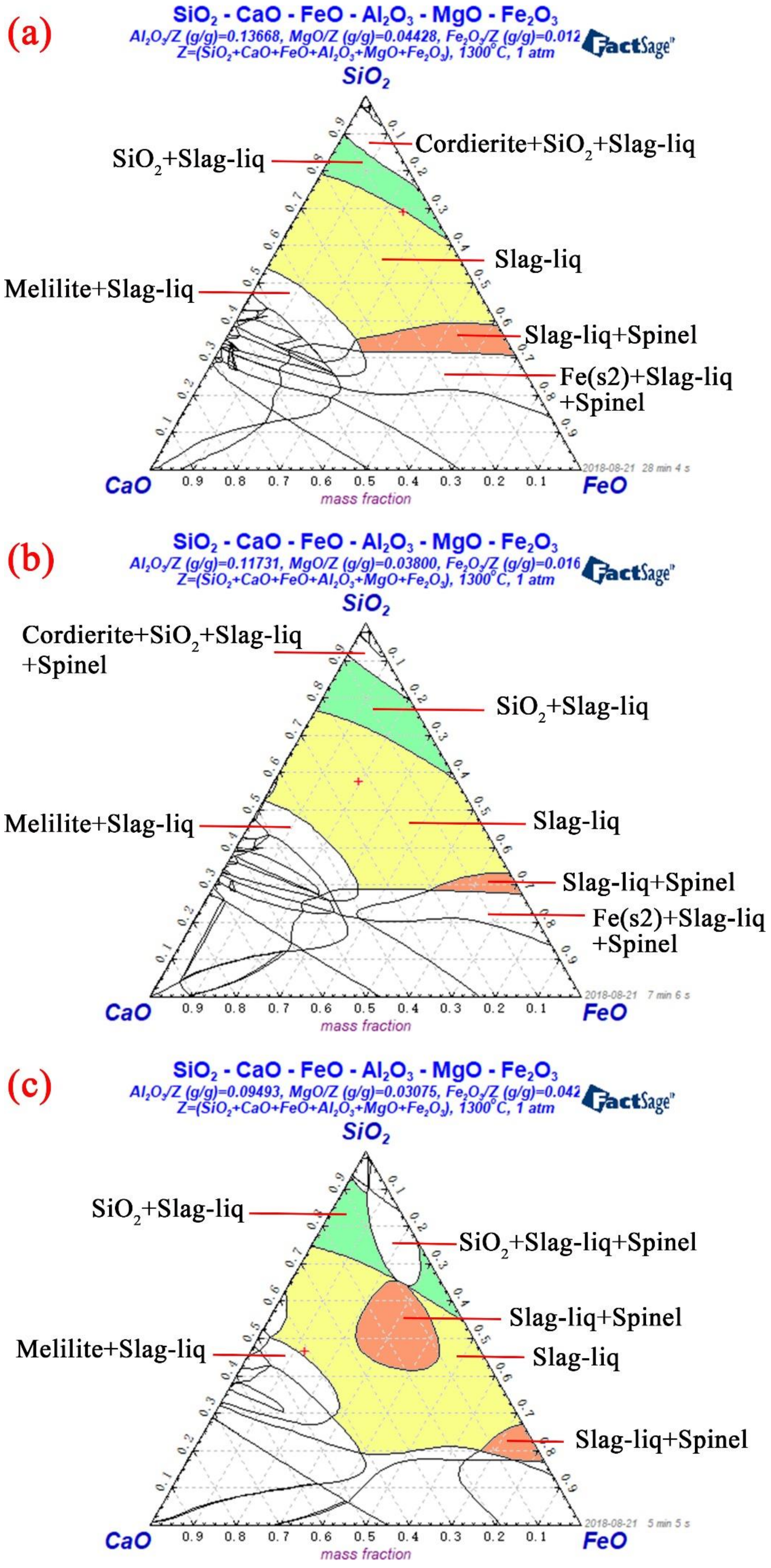
(a)
SiO2 - CaO - FeO - Al2O3 - MgO - Fe2O3
Al2O3/Z (g/g)=0.13668, MgO/Z (g/g)=0.04428, Fe2O3/Z (g/g)=0.012
Z=(SiO2+CaO+FeO+Al2O3+MgO+Fe2O3), 1300°C, 1 atm
FactSage
SiO2
Cordierite+SiO2+Slag-liq
SiO2+Slag-liq
Slag-liq
Melilite+Slag-liq
Slag-liq+Spinel
Fe(s2)+Slag-liq
+Spinel
2018-08-21 28 min 4 s
CaO
FeO
0.9 0.8 0.7 0.6 0.5 0.4 0.3 0.2 0.1
mass fraction
(b)
SiO2 - CaO - FeO - Al2O3 - MgO - Fe2O3
Al2O3/Z (g/g)=0.11731, MgO/Z (g/g)=0.03800, Fe2O3/Z (g/g)=0.016
Z=(SiO2+CaO+FeO+Al2O3+MgO+Fe2O3), 1300°C, 1 atm
FactSage
SiO2
Cordierite+SiO2+Slag-liq
+Spinel
SiO2+Slag-liq
Melilite+Slag-liq
Slag-liq
Slag-liq+Spinel
Fe(s2)+Slag-liq
+Spinel
2018-08-21 7 min 6 s
CaO
FeO
0.9 0.8 0.7 0.6 0.5 0.4 0.3 0.2 0.1
mass fraction
(c)
SiO2 - CaO - FeO - Al2O3 - MgO - Fe2O3
Al2O3/Z (g/g)=0.09493, MgO/Z (g/g)=0.03075, Fe2O3/Z (g/g)=0.042
Z=(SiO2+CaO+FeO+Al2O3+MgO+Fe2O3), 1300°C, 1 atm
FactSage
SiO2
SiO2+Slag-liq
SiO2+Slag-liq+Spinel
Slag-liq+Spinel
Melilite+Slag-liq
Slag-liq
Slag-liq+Spinel
2018-08-21 5 min 5 s
CaO
FeO
0.9 0.8 0.7 0.6 0.5 0.4 0.3 0.2 0.1
mass fraction

Fig.4. Slag phase diagram in direct-to-blister copper smelting of chalcocite at 1300 °C with CaO addition of (a) 1.2%, (b) 5.2%, (c) 11.1%.

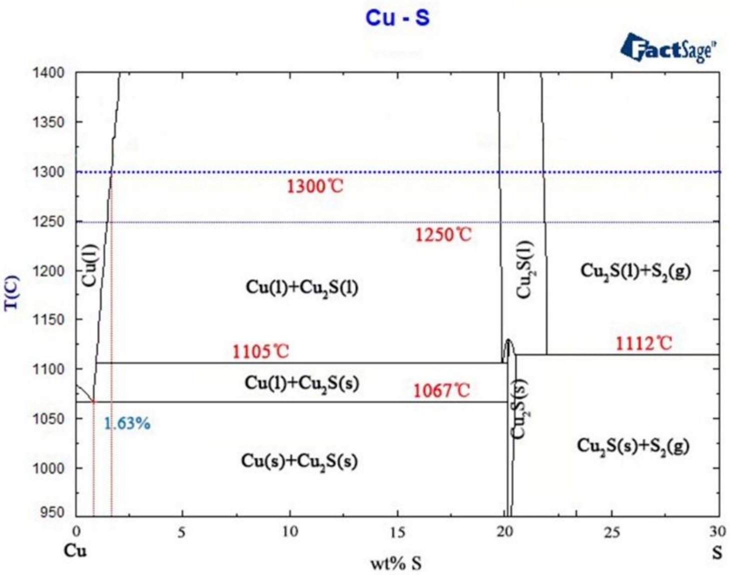

Fig.5. Phase diagram of Cu-S

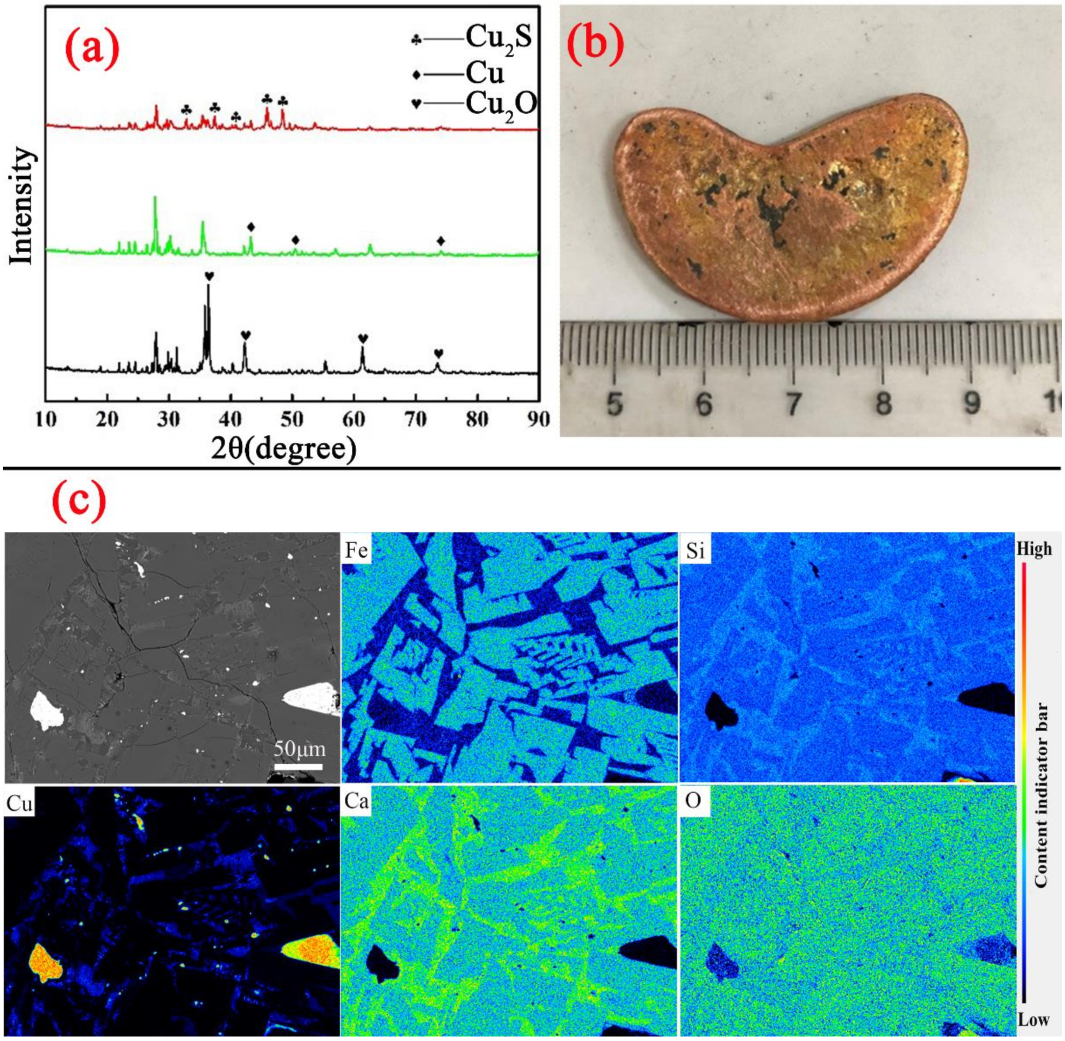

Fig. 6. (a) XRD patterns of copper slag obtained in experiments 2, 5, and 6; (b) Physical map of blister copper in experiment 5; (c) EPMA diagram of copper slag in experiment 5.

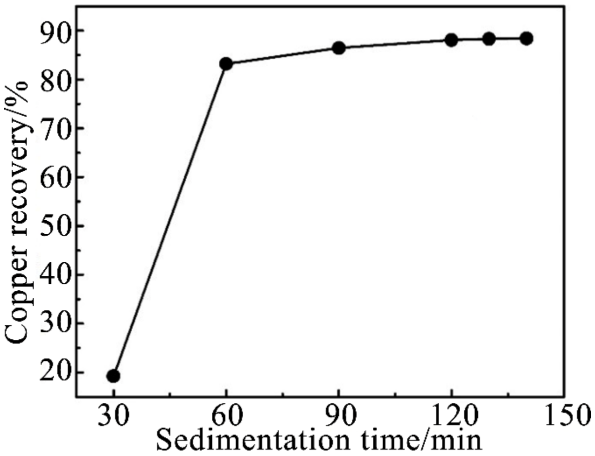

Fig. 7. Effect of sedimentation time on copper recovery.

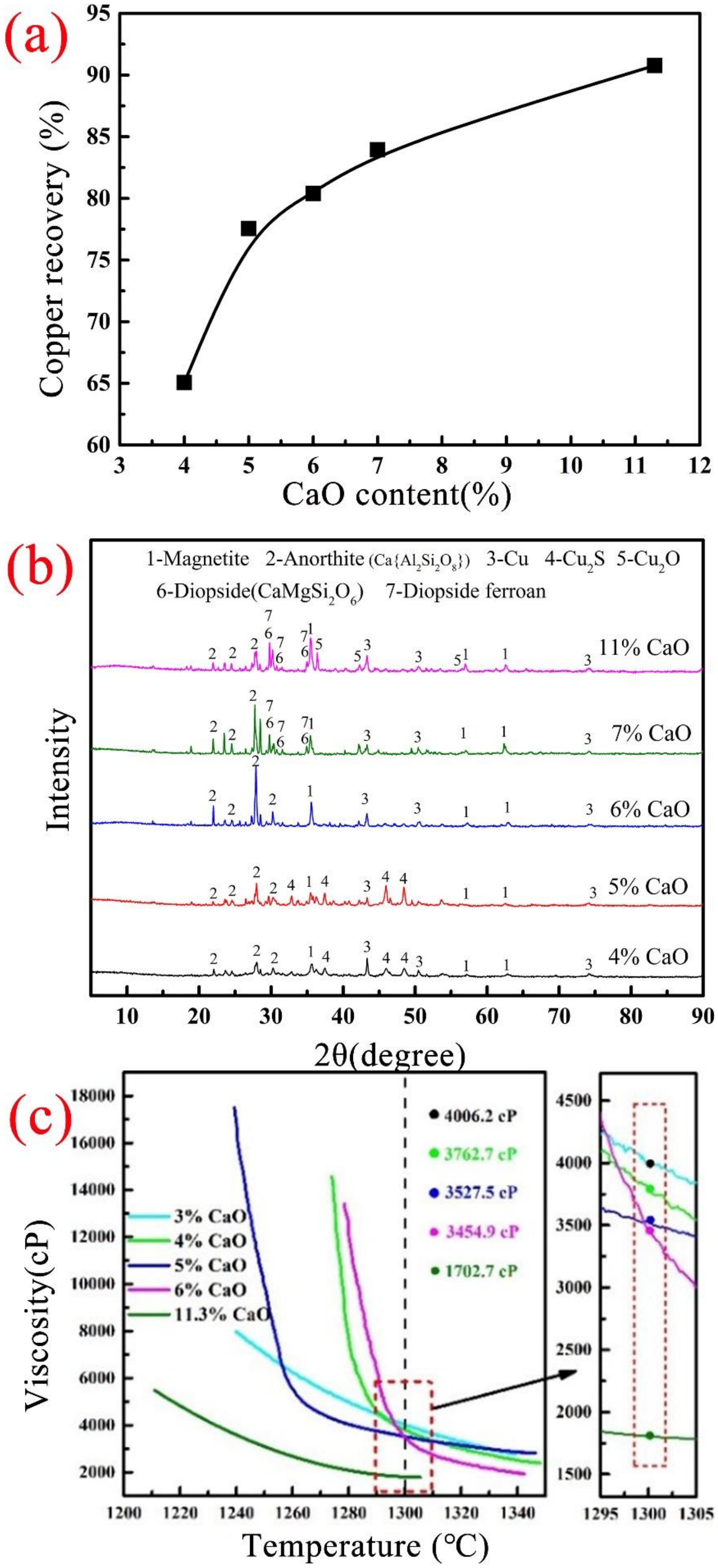

Fig.8. (a) The influence of different CaO additions on copper yield; (b) X-ray diffraction pattern of the slags with different CaO additions; (c) Effect of adding different amounts of CaO to chalcocite on the viscosity of molten slag.

Table 1. Chemical composition of chalcocite raw material.

Element	Cu	Fe	S	SiO_2	CaO	MgO	Al_2O_3
Contents (%)	53.55	4.23	15.26	14.37	0.26	1.15	3.55

Table 2. The effect of CaO addition on smelting parameters.

CaO addition/%	Viscosity/ Pa •s	Sulfur content in blister copper	Copper direct yield /%
1.2	20.62	1.01	95.47
5.2	2.59	1.07	95.67
11.1	0.69	1.44	94.46

Table 3. Chemical composition (%) of the optimal slag type feasibility control scheme.

Fe/SiO_2	Oxygen concentration	Cu	Fe	S	SiO_2	CaO	MgO	Al_2O_3
0.35	21%	46.72	4.39	14.11	12.54	11.49	1	46.72
	50%	46.71	4.39	14.11	12.53	11.51	1	46.71
	70%	46.71	4.39	14.11	12.53	11.51	1	46.71
	85%	46.71	4.39	14.11	12.53	11.51	1	46.71
	99%	46.71	4.39	14.11	12.53	11.51	1	46.71
0.6	21%	45.93	7.4	17.39	12.33	6.37	0.99	45.93
	50%	45.93	7.39	17.39	12.33	6.38	0.99	45.93
	70%	45.93	7.39	17.39	12.32	6.39	0.99	45.93
	85%	45.93	7.39	17.39	12.32	6.39	0.99	45.93
	99%	45.92	7.39	17.39	12.32	6.4	0.99	45.92
0.8	21%	45.16	9.69	19.87	12.12	2.76	0.97	45.16
	50%	44.98	9.66	19.8	12.07	3.13	0.97	44.98
	70%	45.07	9.68	19.83	12.09	2.95	0.97	45.07
	85%	45.07	9.68	19.83	12.09	2.95	0.97	45.07
	99%	45.15	9.69	19.87	12.12	2.77	0.97	45.15

Table 4. Smelting parameters table of the optimal slag type feasibility control scheme.

Fe/SiO_2	Oxygen concentration	S% in blister copper	Blister grade/%	Cu% in slag	Copper direct yield /%	Viscosity/ Pa •s
0.35	21%	0.5	99.35	4.63	95.18	0.564
	50%	0.49	99.26	6.76	93.06	0.57
	70%	0.49	99.21	7.95	91.87	0.574
	85%	0.5	99.16	8.74	91.08	0.575
	99%	0.5	99.12	9.52	90.3	0.576
0.6	21%	0.49	99.36	4.49	95.32	0.513
	50%	0.49	99.26	6.6	93.21	0.526
	70%	0.49	99.21	7.87	91.96	0.533
	85%	0.49	99.17	8.79	91.04	0.538
	99%	0.5	99.12	9.57	90.25	0.542
0.8	21%	0.49	99.36	5.4	94.41	0.485
	50%	0.49	99.26	7.77	92.05	0.493
	70%	0.48	99.22	9.54	90.28	0.496
	85%	0.5	99.16	10.53	89.29	0.503
	99%	0.49	99.13	11.77	88.06	0.527

Table 5. The effect of gas injection time on copper recovery at a 21% oxygen concentration.

Experiment number	Injection time /min	Blister quantity /g	Copper recovery /%
1	90(80.4%)*	12.32	56.4
2	100(89.3%)	19.39	79.8
3	106(94.6%)	22.78	89.2
4	112(100.0%)	23.30	89.7
5	118(105.3%)	23.54	90.5
6	123(109.8%)	22.03	86.3
7	150(133.9%)	5.35	25.1
8	180(160.7%)	0	0

* The numbers in parentheses indicate the ratio of the actual injection time to the theoretical injection time

Table 6. Technical indicators for direct-to-blister copper smelting by adjusting the iron-silicon ratio of chalcocite mixed pyrite to 0.35, 0.6 and 0.8.

	Oxygen concentration	Copper recovery/%	Blister grade/%	Copper content in slag/%	Sulfur content in blister copper/%
0.35	21%	86.56	98.73	13.12	0.48
	50%	93.06	99.35	4.63	0.50
	70%	90.08	98.80	8.38	0.71
	85%	84.62	98.45	14.86	0.47
	99%	83.4	97.25	15.16	0.57
0.6	21%	80.5	98	11.24	0.5
	50%	83.01	97.97	15.82	0.49
	70%	83.46	98.21	13.21	0.46
	85%	80.17	98.94	12.57	0.44
	99%	82.31	98.16	12.82	0.45
0.8	21%	82.79	97.86	13.79	0.51
	50%	85.61	98.21	14.29	0.52
	70%	86.05	98.6	12.18	0.56
	85%	86.79	98	12.73	0.44
	99%	81.78	98.06	15.33	0.63

Biographies

SONG WANG is a doctoral student at the School of Metallurgy of Northeastern University. His main research areas include strategic metal recovery, polymer synthesis, pressurized hydrometallurgy, and clean utilization of non-traditional metallurgical resources.

GUOZHI LV is a professor at Northeastern University, a doctor, a doctoral supervisor, and the deputy director of the Department of Metallurgical Engineering. He is also the deputy director of the Institute of Special Metallurgy and Process Engineering, and is mainly responsible for research related to pressurized hydrometallurgical processes. He has presided over three National Natural Science Foundation projects and participated in more than 20 research projects such as the National Natural Science Foundation key projects and the national "863 Program" key projects as the executive director and research backbone.

TINGAN ZHANG is a second-level professor at Northeastern University, a doctor, a doctoral supervisor, a member of the State Council's academic review group, a recipient of the government's special allowance, and a foreign academician of Russia. He is also the executive director of the China Nonferrous Metals Industry Association and the honorary executive director of the China

Nonferrous Metals Society. He is currently the director of the Engineering Center of the Ministry of Education for Nonferrous Metals Metallurgical Process Technology, the dean of the Nonferrous Metals Solid Waste Technology Research Institute of Northeastern University, and the former dean of the School of Materials and Metallurgy of Northeastern University and the director of the library.